

# Dissociation products and structures of solid H<sub>2</sub>S at strong compression

Yinwei Li,<sup>1</sup> Lin Wang,<sup>2,3</sup> Hanyu Liu,<sup>3,4</sup> Yunwei Zhang,<sup>3</sup> Jian Hao,<sup>1</sup> Chris J. Pickard,<sup>5</sup> Joseph R. Nelson,<sup>6</sup> Richard J. Needs,<sup>6</sup> Wentao Li,<sup>2</sup> Yanwei Huang,<sup>2</sup> Ion Errea,<sup>7,8</sup> Matteo Calandra,<sup>9</sup> Francesco Mauri,<sup>9</sup> and Yanming Ma<sup>3,\*</sup>

<sup>1</sup>*School of Physics and Electronic Engineering, Jiangsu Normal University, Xuzhou 221116, China*

<sup>2</sup>*Center for High Pressure Science and Technology Advanced Research, Shanghai, 201203, China*

<sup>3</sup>*State Key Laboratory of Superhard Materials, Jilin University, Changchun 130012, China*

<sup>4</sup>*Geophysical Laboratory, Carnegie Institution of Washington, Washington D.C. 20015, USA*

<sup>5</sup>*Department of Materials Science & Metallurgy, University of Cambridge,  
27 Charles Babbage Road, Cambridge CB3 0FS, United Kingdom*

<sup>6</sup>*Theory of Condensed Matter Group, Cavendish Laboratory,  
J J Thomson Avenue, Cambridge CB3 0HE, United Kingdom*

<sup>7</sup>*Donostia International Physics Center (DIPC), Manuel de Lardizabal pasealekua 4,  
20018 Donostia-San Sebastián, Basque Country, Spain*

<sup>8</sup>*Fisika Aplikatua 1 Saila, EUITI Bilbao, University of the Basque Country (UPV/EHU),  
Rafael Moreno "Pitxitxi" Pasealekua 3, 48013 Bilbao, Basque Country, Spain*

<sup>9</sup>*IMPMC, UMR CNRS 7590, Sorbonne Universités - UPMC Univ. Paris 06,  
MNHN, IRD, 4 Place Jussieu, F-75005 Paris, France*

Hydrogen sulfides have recently received a great deal of interest due to the record high superconducting temperatures of up to 203 K observed on strong compression of dihydrogen sulfide (H<sub>2</sub>S). A joint theoretical and experimental study is presented in which decomposition products and structures of compressed H<sub>2</sub>S are characterized, and their superconducting properties are calculated. In addition to the experimentally known H<sub>2</sub>S and H<sub>3</sub>S phases, our first-principles structure searches have identified several energetically competitive stoichiometries that have not been reported previously; H<sub>2</sub>S<sub>3</sub>, H<sub>3</sub>S<sub>2</sub>, and H<sub>4</sub>S<sub>3</sub>. In particular, H<sub>4</sub>S<sub>3</sub> is predicted to be thermodynamically stable within a large pressure range of 25–113 GPa. High-pressure room-temperature X-ray diffraction measurements confirm the presence of H<sub>3</sub>S and H<sub>4</sub>S<sub>3</sub> through decomposition of H<sub>2</sub>S that emerge at 27 GPa and coexist with residual H<sub>2</sub>S, at least up to the highest pressure studied in our experiments of 140 GPa. Electron-phonon coupling calculations show that H<sub>4</sub>S<sub>3</sub> has a small  $T_c$  of below 2 K, and that H<sub>2</sub>S is mainly responsible for the observed superconductivity of samples prepared at low temperature (<100K).

PACS numbers: 62.50.-p, 61.50.Ah, 61.05.cp, 74.70.Ad

Superconductivity with a transition temperature  $T_c$  of up to 203 K was observed recently in solid H<sub>2</sub>S at Megabar pressures, which is the highest record among all known superconductors [1]. Ashcroft suggested that metallic hydrogen would be a superconductor at high pressures with a  $T_c$  around room temperature [2], and subsequently predicted that hydrogen-rich metallic compounds might also be superconducting at high pressures [3]. Early theoretical studies focussed on high-pressure silicon and aluminum hydrides [4, 5], and a number of potential high-temperature superconductors have now been proposed in compressed hydrogen-rich compounds, with  $T_c$ s estimated in the range 40–250 K (e.g., GaH<sub>3</sub> [6, 7], SnH<sub>4</sub> [8], GeH<sub>4</sub> [9], NbH<sub>4</sub> [10], Si<sub>2</sub>H<sub>6</sub> [11], SiH<sub>4</sub>(H<sub>2</sub>)<sub>2</sub> [12], CaH<sub>6</sub> [13], YH<sub>3</sub> [14], YH<sub>4</sub> and YH<sub>6</sub> [15]). They have not been realized in practice, in part because of demanding experimental challenges.

The high pressure phase diagram of H<sub>2</sub>S has been studied extensively. H<sub>2</sub>S is a sister molecule of H<sub>2</sub>O, and is the only known stable compound in the H-S system at ambient pressure. High-pressure diamond anvil cell experiments led to the discovery of a metallic phase at about 96 GPa [16–27]. However, partial decomposition of H<sub>2</sub>S and elemental sulfur was observed in Raman [26] and

XRD studies [21] at room temperature above 27 GPa. H<sub>2</sub>S had not been considered as a candidate for superconductivity because it was believed to dissociate into elemental sulfur and hydrogen under high pressures [28]. Recent first-principles structure searches predicted energetically stable metallic structures of H<sub>2</sub>S above 110 GPa [29] and excluded dissociation into its elements. An estimated maximum  $T_c$  for metallic H<sub>2</sub>S of 80 K at 160 GPa was predicted [29]. Motivated by this study, Drozdov *et al.* [1] performed high-pressure experiments on solid H<sub>2</sub>S looking for superconductivity and found an astonishing  $T_c$  of 203 K at 155 GPa [1]. H<sub>2</sub>S shows complex superconducting behavior at high pressures with the emergence of two different superconducting states. Samples prepared at low temperature (100 K) have a  $T_c$  of ~30 K at 110 GPa at the onset of superconductivity, which increases rapidly to a maximum value of 150 K at 200 GPa, while samples at room temperature or above show a maximum  $T_c$  of 203 K at 155 GPa.

Strobel *et al.* synthesized another H-S compound, H<sub>3</sub>S, by compressing a mixture of H<sub>2</sub>S and H<sub>2</sub> above 3.5 GPa [30]. The superconducting  $T_c$  of H<sub>3</sub>S at 200 GPa was recently predicted to be as high as 191–204 K [31], with H<sub>3</sub>S in a cubic Im $\bar{3}$ m structure, which is known already

in  $\text{H}_2\text{O}$  at terapascal pressures [32] through decomposition of  $\text{H}_2\text{O}$ . The agreement between experimental [1] and theoretical values of  $T_c$  [31] led to the proposal by Drozdov *et al.* that  $\text{H}_3\text{S}$  could be formed by decomposition of  $\text{H}_2\text{S}$  and might be responsible for the observed superconducting state at 203 K [1]. This proposal was supported by first-principles density-functional-theory (DFT) studies which suggested that it is thermodynamically favorable for  $\text{H}_2\text{S}$  to decompose into  $\text{H}_3\text{S} + \text{S}$  [33–35] at pressures above 43 GPa [34]. Apparently, there is an urgent need to characterize the decomposition products of compressed  $\text{H}_2\text{S}$  in an effort to build an understanding of the complex superconducting behavior exhibited by the H-S system.

Here we present a joint theoretical and experimental study of compressed  $\text{H}_2\text{S}$  which clarifies the possible decomposition products and their structures. First-principles DFT structure searches were used to predict several new stoichiometries ( $\text{H}_2\text{S}_3$ ,  $\text{H}_3\text{S}_2$ , and  $\text{H}_4\text{S}_3$ ) and a new structure in  $\text{H}_3\text{S}$  not reported previously. Room-temperature high pressure X-ray diffraction (XRD) experiments demonstrate that above 27 GPa,  $\text{H}_2\text{S}$  partially decomposes into  $\text{S} + \text{H}_3\text{S} + \text{H}_4\text{S}_3$ .  $\text{H}_4\text{S}_3$  emerges as the major component at around 66 GPa and coexists with a small fraction of  $\text{H}_3\text{S}$  and residual  $\text{H}_2\text{S}$ , at least up to the highest pressure studied experimentally of 140 GPa.

Extensive structure searches over 44 H-S stoichiometries at 25, 50, 100 and 150 GPa were performed using the CALYPSO [36, 37] and AIRSS [4, 38] methods, which have been successfully used to investigate structures of materials at high pressures [4, 13, 39–45]. The underlying structural relaxations were performed using the Vienna *ab initio* simulation package (VASP) [46] for CALYPSO and the CASTEP plane-wave code [47] for AIRSS. Electron-phonon coupling (EPC) calculations were performed with density functional perturbation theory using the Quantum-ESPRESSO package [48]. XRD data were collected at the 15U1 beamline at the Shanghai Synchrotron Radiation Facility (SSRF) with a monochromatic beam of wavelength 0.6199 Å. The diffraction patterns were integrated with the FIT2D computer code [49] and fitted by Rietveld profile matching using the GSAS+EXPGUI programs [50, 51]. More information about the calculations and experiments is provided in the Supplemental Material [52].

Figure 1 shows convex hull diagrams at 25, 50, 100 and 150 GPa which summarize the results of the structure searches. The effects of including quantum zero-point vibrational motion are significant and they tend to increase with pressure. Our results suggest that up to five H-S compounds lie on the convex hull at some pressures and are therefore thermodynamically stable. Besides the experimentally known  $\text{H}_2\text{S}$  and  $\text{H}_3\text{S}$  compounds, we predict three additional stable compounds:  $\text{H}_4\text{S}_3$ ,  $\text{H}_3\text{S}_2$  and  $\text{H}_2\text{S}_3$ . Note that  $\text{H}_2\text{S}$  is theoretically found to be stable only below 25 GPa, while  $\text{H}_3\text{S}$  appears at all pres-

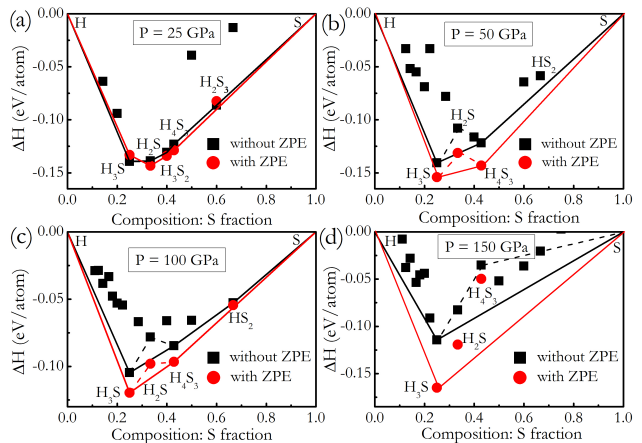


FIG. 1: (Color online) Results from structure searching at 25 (a), 50 (b), 100 (c) and 150 GPa (d). Convex hulls are shown as continuous lines, with (red) and without (black) the inclusion of zero point vibrational enthalpy (ZPE).

sures considered. Enthalpy calculations show that  $\text{H}_3\text{S}$  becomes energetically more stable than  $\text{H}_2\text{S} + 1/2\text{H}_2$  at around 6 GPa. The newly predicted  $\text{H}_3\text{S}_2$  and  $\text{H}_2\text{S}_3$  phases have very narrow pressure ranges of stability and are unstable above 34 and 25 GPa, respectively (Supplemental Material, Fig. S1 [52]). We have therefore omitted further discussion of these compounds. The corresponding crystallographic parameters and phonon dispersion curves are provided in the Supplemental Material [52].

For  $\text{H}_3\text{S}$ , besides the P1, Cccm, R3m and  $\text{Im}\bar{3}\text{m}$  structures of earlier studies [31], our searches predict a monoclinic C2/c structure (4 f.u./cell) that was not reported earlier. The C2/c structure consists of weakly bonded  $\text{H}_2\text{S}$  and  $\text{H}_2$  molecules (Supplemental Material, Fig. S7b [52]), and is calculated to be more stable at pressures of 2–112 GPa than the Cccm structure proposed previously [31] (Supplemental Material, Fig. S7a [52]). Static-lattice enthalpy calculations give a zero-temperature phase sequence for  $\text{H}_3\text{S}$  of P1  $\rightarrow$  C2/c (2 GPa)  $\rightarrow$  R3m (112 GPa)  $\rightarrow$   $\text{Im}\bar{3}\text{m}$  (180 GPa).

$\text{H}_4\text{S}_3$  adopts an orthorhombic  $P2_12_12_1$  (4 f.u./cell) structure that consists of weakly bonded HS and  $\text{H}_2\text{S}$  molecules at 25 GPa (Fig. 2a). The H-S bond lengths within the HS and  $\text{H}_2\text{S}$  molecules are 1.354 Å and 1.387–1.391 Å, respectively, which are significantly shorter than the H-S separation of 1.913–1.932 Å between molecules. With increasing pressure, the neighboring molecules bond with each other forming planar H-S-H-S zigzag chains and puckered H-S-H-S chains, respectively.  $P2_12_12_1$  transforms to a Pnma structure at 60 GPa (Fig. 2c). The convex hull data suggests two synthesis routes for  $\text{H}_4\text{S}_3$ : (i) decomposition of  $8\text{H}_2\text{S} \rightarrow \text{S} + 4\text{H}_3\text{S} + \text{H}_4\text{S}_3$  above 25 GPa; (ii) reaction of  $4\text{H}_3\text{S} + 5\text{S} \rightarrow 3\text{H}_4\text{S}_3$  in the pressure range of 25–113 GPa. Theo-

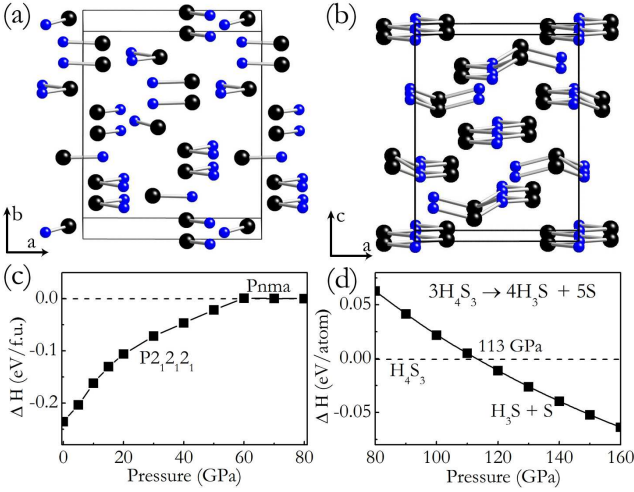


FIG. 2: (Color online) Energetically favorable structures of  $\text{H}_4\text{S}_3$  with space groups  $P2_12_12_1$  (a) and  $Pnma$  (b). Small and large spheres represent H and S atoms, respectively. (c) Calculated enthalpy curves of the  $P2_12_12_1$  structure with respect to the  $Pnma$  structure for  $\text{H}_4\text{S}_3$  as a function of pressure. (d) Decomposition enthalpy curves of  $\text{H}_4\text{S}_3$  into  $(\text{H}_3\text{S} + \text{S})$  as a function of pressure.

retically, it is found that  $\text{H}_4\text{S}_3$  decomposes into  $\text{H}_3\text{S} + \text{S}$  above 113 GPa (Fig. 1d and Fig. 2d).

Powder XRD patterns obtained on increasing pressure from 10 to 140 GPa at room temperature are shown in Fig. 3a. The XRD patterns collected at pressures up to 46 GPa are in excellent agreement with previous data [17–21], and the successive transitions of phase  $\text{I}' \rightarrow$  phase IV  $\rightarrow$  phase V are well reproduced. The XRD data at 10 GPa correspond to phase  $\text{I}'$ . Phase IV with additional peaks at around  $12^\circ$  and  $15^\circ$  (shown by arrows in Fig. 3a) was observed at 16 GPa. The diffraction peaks of phase IV weaken at pressures above 27 GPa, and a new diffraction profile observed at 46 GPa is responsible for phase V. The XRD data show that the IV  $\rightarrow$  V transition begins above 27 GPa, in excellent agreement with previous results [18, 21].

Previous high-pressure Raman [26] and XRD [21] studies have claimed that decomposition of  $\text{H}_2\text{S}$  occurs at room temperature above 27 GPa. Indeed, we found that  $\text{H}_2\text{S}$  partially decomposes in phase V. Unfortunately, we have not found it possible to resolve the decomposition products and their crystal structures from our current XRD data. Therefore we use the predicted structures and convex hull data to help in analysing the experimental data. At 50 GPa, our calculations suggest an energetically allowed dissociation path of  $8\text{H}_2\text{S} \rightarrow \text{S} + 4\text{H}_3\text{S} + \text{H}_4\text{S}_3$  (Fig. 1b). The XRD profile at 46 GPa was therefore fitted to a mixture of  $\text{H}_2\text{S} + \text{S} + \text{H}_3\text{S} + \text{H}_4\text{S}_3$  by performing Rietveld refinements using the most energetically stable structures. Remarkably, we found that the

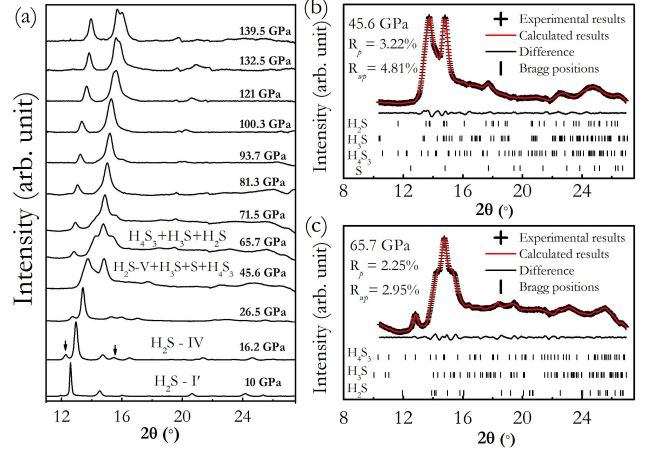


FIG. 3: (Color online) (a) XRD patterns of  $\text{H}_2\text{S}$  collected at various pressures and at room temperature with an incident wavelength of  $0.6199 \text{ \AA}$ . [(b) and (c)] Rietveld refinements of XRD profiles at 45.6 GPa based on the compositions  $\text{Pc-H}_2\text{S}$ ,  $\text{I}_{41}/\text{acd-S}$ ,  $\text{C2/c-H}_3\text{S}$  and  $\text{P2}_12_12_1\text{-H}_4\text{S}_3$  with phase fractions of 1147:85:31:1, and at 65.7 GPa based on compositions of  $\text{Pnma-H}_4\text{S}_3$ ,  $\text{C2/c-H}_3\text{S}$  and  $\text{Pc-H}_2\text{S}$  with phase fractions of 5:3.4:1, respectively. The cross symbols and red solid lines represent observed and fitted patterns, respectively. The solid lines at the bottom are the difference between the observed and fitted patterns. Vertical bars under the pattern represent the calculated positions of reflections arising from the compositions.

XRD profile can be well indexed by a mixture of  $\text{Pc}$ -structured  $\text{H}_2\text{S}$ ,  $\text{I}_{41}/\text{acd}$ -structured  $\text{S}$ ,  $\text{C2/c}$ -structured  $\text{H}_3\text{S}$  and  $\text{P2}_12_12_1$ -structured  $\text{H}_4\text{S}_3$ , with phase fractions (ratios of numbers of unit cells) of 1147:85:31:1, as shown in Fig. 3b. The existence of a large proportion of  $\text{H}_2\text{S}$  demonstrates the partial decomposition. We also attempted other Rietveld refinements fitting the XRD patterns to pure  $\text{H}_2\text{S}$ ,  $\text{H}_2\text{S} + \text{S} + \text{H}_3\text{S}$  or  $\text{S} + 4\text{H}_3\text{S} + \text{H}_4\text{S}_3$ , but all of these fits gave poorer results (Supplemental Material, Fig. S10 [46]). The calculated decomposition pressure (30 GPa) for  $8\text{H}_2\text{S} \rightarrow \text{S} + 4\text{H}_3\text{S} + \text{H}_4\text{S}_3$  (Supplemental Material, Fig. S13 [52]) is in excellent agreement with the value of 27 GPa observed in experiment [21].

With increasing pressure, more  $\text{H}_2\text{S}$  decomposes and its contribution to the XRD signal is reduced. The XRD pattern collected at 66 GPa shows entirely different features to that at 46 GPa. Rietveld refinement shows that a mixture of  $\text{Pnma}$ -structured  $\text{H}_4\text{S}_3$ ,  $\text{C2/c}$ -structured  $\text{H}_3\text{S}$ , and  $\text{Pc}$ -structured  $\text{H}_2\text{S}$  with phase fractions 5:3.4:1 gives the best fit to the experimental data (Fig. 3c). The disappearance of elemental  $\text{S}$  and the reduction in the ratio of  $\text{H}_3\text{S}$  are understandable since a reaction of  $4\text{H}_3\text{S} + 5\text{S} \rightarrow 3\text{H}_4\text{S}_3$  takes place as inferred from our convex hull calculations (Fig. 1b and 1c). The two shoulders on the main peak at  $15^\circ$  originate primarily from  $\text{H}_3\text{S}$  and  $\text{H}_2\text{S}$ . These shoulders weaken when the pressure is increased



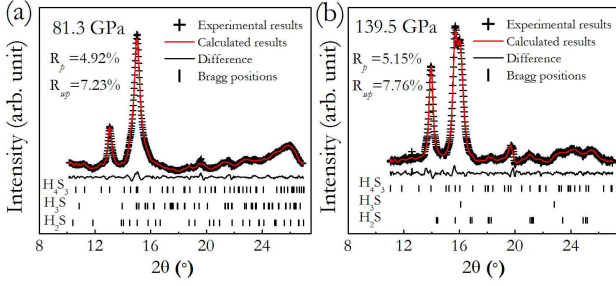


FIG. 4: (Color online) Rietveld refinements of XRD profiles at 81.3 GPa based on Pnma-H<sub>4</sub>S<sub>3</sub> + C2/c-H<sub>3</sub>S + Pmc2<sub>1</sub>-H<sub>2</sub>S with phase fractions of 43:6:1 (a) and at 139.5 GPa based on Pnma-H<sub>4</sub>S<sub>3</sub> + R3m-H<sub>3</sub>S + P-1-H<sub>2</sub>S with phase fractions of 56:7:1 (c).

to 82 GPa and the XRD pattern can then be well indexed by Pnma-structured H<sub>4</sub>S<sub>3</sub>, C2/c-structured H<sub>3</sub>S and Pmc2<sub>1</sub>-structured H<sub>2</sub>S with a major contribution (86%) from H<sub>4</sub>S<sub>3</sub> (Fig. 4a). Our results demonstrate that H<sub>4</sub>S<sub>3</sub> coexists with H<sub>3</sub>S and H<sub>2</sub>S at least up to 140 GPa, the highest pressure studied experimentally (Fig. 4b). At this pressure, a refinement based on Pnma-structured H<sub>4</sub>S<sub>3</sub> and C2/c-structured H<sub>3</sub>S leads to poorer fits with higher  $R_p$  and  $R_{wp}$  values (Supplemental Material, Fig. S12 [52]), which supports the existence of residual H<sub>2</sub>S (about 1.6%).

H<sub>4</sub>S<sub>3</sub> becomes metallic at 102 GPa (Supplemental Material, Fig. S14 [52]). However, the calculated electron-phonon-coupling parameter ( $\lambda = 0.42$ ) is very small at 140 GPa due to the low density of states at the Fermi level of 0.09 eV<sup>-1</sup>/atom. As a result, the  $T_c$  estimated from the Allen and Dynes modified McMillan equation [53] with  $\mu^*$  of 0.16–0.13 is only 0.75–2.1 K at 140 GPa.

In Fig. 5, we compare the calculated  $T_c$  values for H<sub>4</sub>S<sub>3</sub>, H<sub>2</sub>S and H<sub>3</sub>S to experimental data measured in compressed H<sub>2</sub>S [1], where  $T_c$  obtained for samples prepared at low and high temperatures are denoted by L- $T_c$  and H- $T_c$ , respectively. On the one hand, the observed L- $T_c$  [1] at pressures below 160 GPa can only be quantitatively reproduced by H<sub>2</sub>S, while the nature of the rapidly increasing L- $T_c$  above 160 GPa remains unclear because the calculated  $T_c$  values of H<sub>3</sub>S, H<sub>4</sub>S<sub>3</sub>, and H<sub>2</sub>S are too high, too low, and tending to decrease, respectively. On the other hand, although the values of  $T_c$  for Im3m structured H<sub>3</sub>S calculated within the harmonic approximation are much higher than the observed H- $T_c$  [54], the inclusion of anharmonic effects reproduces the H- $T_c$  data above 180 GPa [35] quite well. However, at low pressures around 150 GPa,  $T_c$  values [54] estimated for R3m-H<sub>3</sub>S within the harmonic approximation are ~45 K lower than the observed H- $T_c$ . Meanwhile, the predicted  $T_c$  for R3m-H<sub>3</sub>S increases with pressure, in stark contrast to the experimental observation of a decrease in

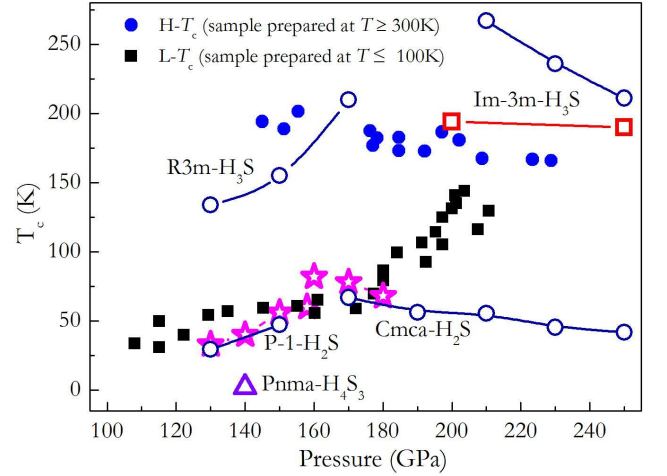


FIG. 5: (Color online) Superconducting transition temperatures ( $T_c$ ) calculated for various H-S compounds and experimental values for compressed H<sub>2</sub>S [1]. Solid squares and circles show experimental data from Fig. 1(b) and Fig. 2 (b) of Ref. 1, respectively, where different runs are represented by the same symbols. The open stars, squares and circles show calculated data from Ref. 29, Ref. 35 and Ref. 54, respectively. Open triangles denote calculated  $T_c$  for Pnma-H<sub>4</sub>S<sub>3</sub> in the present study. Note that the  $T_c$  values (open squares) for Im3m-H<sub>3</sub>S taken from Ref. 35 include anharmonic effects, while all other estimated  $T_c$ s are calculated within the harmonic approximation.

H- $T_c$ . Apparently, further study is greatly needed to disclose the steep  $T_c$  increase of L- $T_c$  above 160 GPa and the high H- $T_c$  at around 150 GPa.

We find that kinetics plays an important role in determining the experimentally observed H-S structures. Theory suggests that H<sub>2</sub>S and H<sub>4</sub>S<sub>3</sub> decompose above 25 and 113 GPa (Supplemental Material Fig. S13 and Fig. 2d), respectively. However, H<sub>2</sub>S and H<sub>4</sub>S<sub>3</sub> are observed to persist up to at least 140 GPa. Large kinetic barriers must therefore play a major role in suppressing decomposition at high pressures, as has been found in other materials [55–58].

In summary, through first-principles structure searching calculations, we predict three new stable H-S compounds with stoichiometries H<sub>3</sub>S<sub>2</sub>, H<sub>2</sub>S<sub>3</sub>, and H<sub>4</sub>S<sub>3</sub> and a new C2/c structure of H<sub>3</sub>S, enriching the phase diagram of H-S systems at high pressures. The formation of H<sub>4</sub>S<sub>3</sub> and H<sub>3</sub>S was confirmed by XRD experiments to occur through decomposition of compressed H<sub>2</sub>S above 27 GPa resulting in the products S + H<sub>3</sub>S + H<sub>4</sub>S<sub>3</sub>. H<sub>4</sub>S<sub>3</sub> becomes a major component at around 66 GPa and is stable up to at least 140 GPa, with a small fraction of H<sub>3</sub>S and residual H<sub>2</sub>S. We have also examined potential superconductivity of metallic H<sub>4</sub>S<sub>3</sub> via explicit calculations of electron-phonon coupling parameters and the superconducting  $T_c$ . Our work suggests that kinetically

protected  $\text{H}_2\text{S}$  in samples prepared at low temperature is responsible for the observed superconductivity below 160 GPa.

Y. L. and J. H. acknowledge funding from the National Natural Science Foundation of China under Grant No. 11204111 and No. 11404148, the Natural Science Foundation of Jiangsu province under Grant No. BK20130223, and the PAPD of Jiangsu Higher Education Institutions. Y. Z. and Y. M. acknowledge funding from the National Natural Science Foundation of China under Grant Nos. 11274136 and 11534003, the 2012 Changjiang Scholars Program of China. R. J. N. acknowledges financial support from the Engineering and Physical Sciences Research Council (EPSRC) of the U.K. [EP/J017639/1]. Calculations were performed on the Cambridge High Performance Computing Service facility and the HEC-ToR and Archer facilities of the U.K.'s national high-performance computing service (for which access was obtained via the UKCP consortium [EP/K013564/1]). J. R. N. acknowledges financial support from the Cambridge Commonwealth Trust. I. E. acknowledges financial support from the Spanish Ministry of Economy and Competitiveness (FIS2013-48286-C2-2-P). M. C. acknowledges support from the Graphene Flagship and Agence nationale de la recherche (ANR), Grant No. ANR-13-IS10-0003-01. Work at Carnegie was partially supported by EFree, an Energy Frontier Research Center funded by the DOE, Office of Science, Basic Energy Sciences under Award No. DE-SC-0001057 (salary support for H. L.). The infrastructure and facilities used at Carnegie were supported by NNSA Grant No. DE-NA-00006, CDAC.

---

\* Electronic address: [mym@jlu.edu.cn](mailto:mym@jlu.edu.cn)

- [1] A. P. Drozdov, M. I. Erements, I. A. Troyan, V. Ksenofontov, and S. I. Shylin, *Nature* (2015). Advance online publication, [doi:10.1038/nature14964](https://doi.org/10.1038/nature14964).
- [2] N. W. Ashcroft, *Phys. Rev. Lett.* **21**, 1748 (1968).
- [3] N. W. Ashcroft, *Phys. Rev. Lett.* **92**, 187002 (2004).
- [4] C. J. Pickard and R. J. Needs, *Phys. Rev. Lett.* **97**, 045504 (2006).
- [5] C. J. Pickard and R. J. Needs, *Phys. Rev. B* **76**, 144114 (2007).
- [6] G. Gao, H. Wang, A. Bergara, Y. Li, G. Liu, and Y. Ma, *Phys. Rev. B* **84**, 064118 (2011).
- [7] R. Szcześniak and A. Durajski, *Supercond. Sci. Technol.* **27**, 015003 (2014).
- [8] G. Gao, A. R. Oganov, P. Li, Z. Li, H. Wang, T. Cui, Y. Ma, A. Bergara, A. O. Lyakhov, T. Iitaka, and G. Zou, *Proc. Nat. Acad. Sci. U.S.A.* **107**, 1317 (2010).
- [9] G. Gao, A. R. Oganov, A. Bergara, M. Martinez-Canales, T. Cui, T. Iitaka, Y. Ma, and G. Zou, *Phys. Rev. Lett.* **101**, 107002 (2008).
- [10] A. P. Durajski, *Eur. Phys. J. B* **87**, 211 (2014).
- [11] X. Jin, X. Meng, Z. He, Y. Ma, B. Liu, T. Cui, G. Zou, and H. Mao, *Proc. Nat. Acad. Sci. U.S.A.* **107**, 9969 (2010).
- [12] Y. Li, G. Gao, Y. Xie, Y. Ma, T. Cui, and G. Zou, *Proc. Nat. Acad. Sci. U.S.A.* **107**, 15708 (2010).
- [13] H. Wang, S. T. John, K. Tanaka, T. Iitaka, and Y. Ma, *Proc. Nat. Acad. Sci. U.S.A.* **109**, 6463 (2012).
- [14] D. Y. Kim, R. H. Scheicher, and R. Ahuja, *Phys. Rev. Lett.* **103**, 077002 (2009).
- [15] Y. Li, J. Hao, H. Liu, S. T. John, Y. Wang, and Y. Ma, *Scientific Reports* **5**, 09948 (2015).
- [16] H. Shimizu, Y. Nakamichi, and S. Sasaki, *J. Chem. Phys.* **95**, 2036 (1991).
- [17] S. Endo, N. Ichimiya, K. Koto, S. Sasaki, and H. Shimizu, *Phys. Rev. B* **50**, 5865 (1994).
- [18] S. Endo, A. Honda, S. Sasaki, H. Shimizu, O. Shimomura, and T. Kikegawa, *Phys. Rev. B* **54**, R717 (1996).
- [19] S. Endo, A. Honda, K. Koto, O. Shimomura, T. Kikegawa, and N. Hamaya, *Phys. Rev. B* **57**, 5699 (1998).
- [20] H. Fujihisa, H. Yamawaki, M. Sakashita, K. Aoki, S. Sasaki, and H. Shimizu, *Phys. Rev. B* **57**, 2651 (1998).
- [21] H. Fujihisa, H. Yamawaki, M. Sakashita, A. Nakayama, T. Yamada, and K. Aoki, *Phys. Rev. B* **69**, 214102 (2004).
- [22] M. Sakashita, H. Yamawaki, H. Fujihisa, K. Aoki, S. Sasaki, and H. Shimizu, *Phys. Rev. Lett.* **79**, 1082 (1997).
- [23] H. Shimizu and S. Sasaki, *Science* **257**, 514 (1992).
- [24] H. Shimizu, H. Yamaguchi, S. Sasaki, A. Honda, S. Endo, and M. Kobayashi, *Phys. Rev. B* **51**, 9391 (1995).
- [25] H. Shimizu, T. Ushida, S. Sasaki, M. Sakashita, H. Yamawaki, and K. Aoki, *Phys. Rev. B* **55**, 5538 (1997).
- [26] J. Loveday, R. Nemes, S. Klotz, J. Besson, and G. Hamel, *Phys. Rev. Lett.* **85**, 1024 (2000).
- [27] M. Sakashita, H. Fujihisa, H. Yamawaki, and K. Aoki, *The Journal of Physical Chemistry A* **104**, 8838 (2000).
- [28] R. Rousseau, M. Boero, M. Bernasconi, M. Parrinello, and K. Terakura, *Phys. Rev. Lett.* **85**, 1254 (2000).
- [29] Y. Li, J. Hao, H. Liu, Y. Li, and Y. Ma, *J. Chem. Phys.* **140**, 174712 (2014).
- [30] T. A. Strobel, P. Ganesh, M. Somayazulu, P. R. C. Kent, and R. J. Hemley, *Phys. Rev. Lett.* **107**, 255503 (2011).
- [31] D. Duan, Y. Liu, F. Tian, D. Li, X. Huang, Z. Zhao, H. Yu, B. Liu, W. Tian, and T. Cui, *Scientific Reports* **4**, 6968 (2014).
- [32] C. J. Pickard, M. Martinez-Canales, and R. J. Needs, *Phys. Rev. Lett.* **110**, 245701 (2013).
- [33] N. Bernstein, C. S. Hellberg, M. D. Johannes, I. I. Mazin, and M. J. Mehl, *Phys. Rev. B* **91**, 060511(R) (2015).
- [34] D. Duan, X. Huang, F. Tian, D. Li, H. Yu, Y. Liu, Y. Ma, B. Liu, and T. Cui, *Phys. Rev. B* **91**, 180502 (2015).
- [35] I. Errea, M. Calandra, C. J. Pickard, J. R. Nelson, R. J. Needs, Y. Li, H. Liu, Y. Zhang, Y. Ma, and F. Mauri, *Phys. Rev. Lett.* **114**, 157004 (2015).
- [36] Y. Wang, J. Lv, L. Zhu, and Y. Ma, *Phys. Rev. B* **82**, 094116 (2010).
- [37] Y. Wang, J. Lv, L. Zhu, and Y. Ma, *Comput. Phys. Commun.* **183**, 2063 (2012).
- [38] C. J. Pickard and R. J. Needs, *J. Phys.: Condens. Matter* **23**, 053201 (2011).
- [39] L. Zhu, H. Wang, Y. Wang, J. Lv, Y. Ma, Q. Cui, Y. Ma, and G. Zou, *Phys. Rev. Lett.* **106**, 145501 (2011).
- [40] Y. Wang, H. Liu, J. Lv, L. Zhu, H. Wang, and Y. Ma, *Nat. Commun.* **2**, 563 (2011).
- [41] C. J. Pickard and R. J. Needs, *J. Chem. Phys.* **127**, 244503 (2007).
- [42] C. J. Pickard and R. J. Needs, *Nat. Phys.* **3**, 473 (2007).
- [43] J. M. McMahon and D. M. Ceperley, *Phys. Rev. Lett.*

- [106](#), [165302](#) (2011).
- [44] C. J. Pickard, M. Martinez-Canales, and R. J. Needs, [Phys. Rev. B](#) **85**, [214114](#) (2012).
  - [45] Y. Li, Y. Wang, C. J. Pickard, R. J. Needs, Y. Wang, and Y. Ma, [Phys. Rev. Lett.](#) **114**, [125501](#) (2015).
  - [46] G. Kresse and J. Furthmüller, [Phys. Rev. B](#) **54**, [11169](#) (1996).
  - [47] S. J. Clark, M. D. Segall, C. J. Pickard, P. J. Hasnip, M. I. Probert, K. Refson, and M. C. Payne, [Z. Kristallogr.](#) **220**, [567](#) (2005).
  - [48] P. Giannozzi, S. Baroni, N. Bonini, M. Calandra, R. Car, C. Cavazzoni, D. Ceresoli, G. L. Chiarotti, M. Cococcioni, I. Dabo *et al*, [J. Phys.: Condens. Matter](#) **21**, [395502](#) (2009).
  - [49] A. L. Ruoff, H. Luo, C. Vanderborgh, H. Xia, K. Brister, and V. Arnold, [Rev. Sci. Instrum.](#) **64**, [3462](#) (1993).
  - [50] A. C. Larson and R. B. Von Dreele, General Structure Analysis System. LANSCE, MS-H805, Los Alamos, New Mexico (1994).
  - [51] B. H. Toby, [J. Appl. Cryst.](#) **34**, [210](#) (2001).
  - [52] Reserved for EPAPS.
  - [53] P. B. Allen and R. C. Dynes, [Phys. Rev. B](#) **12**, [905](#) (1975).
  - [54] R. Akashi, M. Kawamura, S. Tsuneyuki, Y. Nomura, and R. Arita, [Phys. Rev. B](#) **91**, [224513](#) (2015).
  - [55] A. R. Oganov, in [Boron Rich Solids](#) (Springer, 2011), pp. [207](#).
  - [56] G. Gao, A. R. Oganov, Y. Ma, H. Wang, P. Li, Y. Li, T. Iitaka, and G. Zou, [J. Chem. Phys.](#) **133**, [144508](#) (2010).
  - [57] P. Kroll, T. Schröter, and M. Peters, [Angew. Chem. Int. Ed.](#) **44**, [4249](#) (2005).
  - [58] X. Zhong, Y. Wang, F. Peng, H. Liu, H. Wang, and Y. Ma, [Chemical Science](#) **5**, [3936](#) (2014).